Experimental validation of variance estimation in the Statistical Energy Analysis of a structural-acoustic system

J Mechanical Engineering Science

www.sagepub.com/
SAGE

Luis Andrade A.[1], Robin S. Langley[1],Tore Butlin[1], Matthew de Brett[1] and Ole M. Nielsen[2]

Abstract

The Statistical Energy Analysis (SEA) approach has largely been used in vibro-acoustic modelling to predict the averaged energy in coupled vibrating structures and acoustic cavities. The average is performed over an ensemble of nominally identical built-up systems where random responses are observed at high frequencies after excitation. Over the years, this approach has been extended to predict the energy variance employing the statistics of the Gaussian Orthogonal Ensemble (GOE), and numerical and experimental evidence has supported the predictions of the mean and variance of energy of coupled vibrating structures. However, little experimental evidence is found to validate the prediction of the variance of energy in coupled structural-acoustic systems. In this work, the mean and variance of energies predicted from an SEA model have been validated with experimental measurements on a structural-acoustic system, comprised by a flat thin plate coupled to an enclosed acoustic volume. The structural system has been randomised by adding small masses on arbitrary positions on the plate, whereas the randomisation of the acoustic cavity is achieved by allocating rigid baffles in random positions within the acoustic volume. In general, good agreement is found between the predictions of the model and the experimental results.

Keywords

Statistical Energy Analysis, Structure-borne sound, Energy variance, GOE statistics, Random vibrations.

Introduction

The response of structural or acoustic systems can be estimated from numerical models, such as the Finite Element Method (FE). However, despite the effectiveness of such numerical approaches to compute the response of a system at a relatively high degree of precision, two major issues arise when modelling a complex vibro-acoustic system. Firstly, it is not feasible to use an FE analysis when a system has to be discretised in an extremely large number of degrees of freedom (DOF) due to the computational cost[1]. In fact, in the analysis at high frequencies, an excessive number of DOF are required to model the short wavelength response, which is a common problem in structure-borne sound, and the analysis turns out to be time consuming and inpractical for modelling real complex structures that might need tens or hundreds of million DOF[2]. Secondly, experimental evidence has shown that the response in the frequency domain is sensitive to uncertainties that might arise from measurements, material properties, manufacturing issues, slight variation of geometries or environmental conditions, among others, and therefore the response of several nominally identical systems is uncertain at high frequencies[3]. Statistical Energy Analysis (SEA) overcomes the impractical issues of deterministic methods, and allows computing the averaged energy over an ensemble of nominally identical systems, being particularly applied for random noise and vibration problems that are linked to the prediction of averaged sound pressure levels[4]. Over the years, there has been much interest in investigating the statistics of structural and acoustic systems to extend the capability of SEA to predict higher degree statistics, such as the variance of energy of the subsystems that comprise a built-up complex system.

The analysis of the statistics in room acoustics has been previously addressed by Schroeder[5]. Considering the point-to-point transfer function, the author has concluded that, at high frequencies, the modulus squared of the transfer function has an exponential distribution, and therefore the standard deviation of energies is equal to the mean energy. Further works carried out independently by Lyon[6] and Davy[7], have considered that the natural frequencies of a complex system form a Poisson point process. However, Langley and Brown[8], point out that the computation of the variance with the latter assumption is over-predicted and invalid for most complex dynamical systems, i.e. irregular and with random boundaries. In Refs.[8,9], the statistics of the Gaussian Orthogonal Ensemble (GOE) have been employed to accurately predict the variance of energies in systems that are sufficiently random for the statistical overlap[10] be greater than one, i.e. there is enough randomness for the natural frequencies to move more than the average frequency spacing over an ensemble.

As it is of interest to determine the statistics of individual subsytems that comprise a complex built-up system, Langley

[1]University of Cambridge, UK
[2]Bose Corporation, USA

Corresponding author:
Luis Andrade A., University of Cambridge, Department of Engineering, Trumpington Street, Cambridge, CB2 1PZ, UK.
Email: lga23@cam.ac.uk

and Cotoni[11] have extended the application of the GOE statistics to predict the variance of energy in complex built-up systems, and there has been shown that the predictions agree very well with the results from numerical simulations. Cotoni et. al.[12] have presented numerical and experimental data to validate the predictions of the energy and variance at a point of several structural subsystems that comprise a built-up structure. Further experimental evidence has supported the application of GOE statistics in room acoustics[13], however, very little can be found in the literature regarding the prediction, and supporting experimental evidence, of the variance of energy in coupled structural-acoustic systems using the GOE statistics. Hence, the aim of the present work is to validate an SEA model of a structural-acoustic system with experimental data of the response of a randomised physical built-up system.

Mean energy response and variance prediction

General form of the SEA equation

A built-up system can be comprised by weakly coupled structural and/or acoustic subsystems, allowing the waves in a vibrating subsystem to be weakly transmitted to another. The vibrating energy due to elastic waves on each subsystem can be both dissipated by internal damping and interchanged between two coupled subsystems through the coupling interface. Such interface can be a connection through points, lines or surfaces[14]. The common form of the SEA equation can be derived from the power balance on the j^{th} subsystem that is connected to N subsystems, and expressed as

$$P_j = \omega\eta_j E_j + \sum_k \omega\eta_{jk} n_j \left(\frac{E_j}{n_j} - \frac{E_k}{n_k}\right),\ k = 1, 2, 3...N \tag{1}$$

where the loss factor, η_j, can be found from tabulated or experimental data. The parameters η_{jk} and n_j are the coupling loss factor and modal density, respectively, and can be found from experiments, numerical simulations or analytical formulas. The power input into the j^{th} subsystem, P_j, is dissipated at a rate described by the term $\omega\eta_j E_j$, and interchanged between the j^{th} and k^{th} coupled subsystems at the rate expressed by the summation in equation (1). The SEA equation extended for all of the N interconnected subsystems can be expressed in the matrix form $\mathbf{C}\hat{\mathbf{E}} = \mathbf{P}$, where the vector $\mathbf{P}$ contains the external power going into each subsystem, $\hat{\mathbf{E}}$ is the vector of the modal energies, i.e. E_j/n_j, and the entries of the $N \times N$ matrix $\mathbf{C}$ are

$$C_{jj} = \omega\left(\eta_j + \sum_{k\neq j}\eta_{jk}\right) n_j \quad \text{and} \tag{2}$$

$$C_{jk} = -\omega\eta_{jk} n_j,\ j \neq k. \tag{3}$$

Variance of energies

The variance of energy of a system might arise due to the spatial distribution of the sources of excitation, the variation on the number of resonant modes, fluctuation in the strength of coupling and the randomness of the position at which the response is measured. The assumption that the natural frequencies conform to the GOE statistics applies to a system that does not have symmetries, such as parallel edges, but any irregularity in the shape or imperfection of the material will reduce such symmetries and the GOE statistics will naturally arise[8,9].

Statistics of a single random system

Based on the GOE statistics, Langley and Brown[8] have developed an expression to compute the relative variance of energies, i.e. the variance over the mean energy squared $r^2 = \text{Var}[E]/\text{E}[E]^2$, of a single random system subjected to harmonic excitation, and can be expressed as

$$r^2(\alpha, m) = \frac{1}{\pi m}\left\{\alpha - 1 + \frac{1}{2\pi m}\left[1 - \exp\left(-2\pi m\right)\right] + \text{E}_{\text{I}}\left(\pi m\right)\left[\cosh\left(\pi m\right) - \frac{1}{\pi m}\sinh\left(\pi m\right)\right]\right\}, \tag{4}$$

where $m = \omega\eta n$ is the modal overlap factor, E_{I} is the exponential integral[15], and α is a parameter that takes into account the statistics of the modal response, i.e. the coefficient of the n^{th} term in the modal expansion of the energy response, a_n, and is given by

$$\alpha = \frac{\text{E}[a_n^2]}{\text{E}[a_n]^2} = \frac{K-2}{N_p} + 2, \tag{5}$$

where K depends on higher order statistics of the mode shapes ϕ_n, i.e. $K = \text{E}[\phi_n^4]/\text{E}[\phi_n^2]^2$. For Gaussian mode shapes K is equal to 3, however, numerical results have found that $K = 2.75$ is a better approximation for plate systems, whereas for acoustic systems $K = 27/8$[8]. N_p is the number of uncorrelated points on which the force is applied. For $N_p = 1$, then $\alpha = K$, while at the limit $N_p \to \infty$, i.e. rain-on-the-roof loading, $\alpha = 2$.

Langley and Brown[9] have extended the analysis to determine the statistics of band-averaged energy, by employing the same GOE statistics, and considering the energy averaged over a frequency band $[\omega - \Delta/2, \omega + \Delta/2]$. Assuming that the loading is approximately constant over this band and $\Delta \ll \omega$, the relative variance is expressed as

$$r^2(\alpha, m, B) = \frac{\alpha - 1}{\pi m}\left(\frac{1}{B^2}\right)\left\{2B\left[\frac{\pi}{2} - \tan^{-1}\left(\frac{1}{B}\right)\right] - \ln\left(1 + B^2\right)\right\} + \frac{1}{(\pi m)^2}\left(\frac{1}{B^2}\right)\ln\left(1 + B^2\right), \tag{6}$$

where B is the bandwidth parameter defined as $B = \Delta/\omega\eta$. As this parameter tends to zero, the relative variance of the kinetic energy is reduced to[9]

$$r^2(\alpha, m) \approx \frac{(\alpha - 1)}{\pi m} + \frac{1}{(\pi m)^2}, \tag{7}$$

which is an approximation of equation (4).

Statistics of a built-up random system

In addition to the prediction of the mean energy, the variance of each subsystem that comprises a complex system

can be estimated by employing the GOE statistics in the SEA equation. Considering that the matrix **C** and the vector **P** of the matrix form of the SEA equation are random quantities, Langley and Cotoni [11] have derived an expression that correlates the variance of energy of the j^{th} subsystem to the variance of the random components of the power input and the random SEA matrix in the form

$$\text{Var}\left[\hat{E}_j\right] = \sum_k \left(C_{jk}^{-1}\right)^2 \text{Var}\left[P_{\text{ran},k}\right] + \sum_k \sum_{s\neq k} \left[\left(C_{jk}^{-1} - C_{js}^{-1}\right)\hat{E}_s\right]^2 \text{Var}\left[C_{\text{ran},ks}\right], \tag{8}$$

where the quantity C_{jk}^{-1} is the jk^{th} entry of the inverse SEA matrix **C**, that is also equal to the ensemble average of the random matrix [12], and $\hat{E}_s$ is the ensemble averaged modal energy that can be computed from the SEA equation of the system. The variance of the fluctuations of the input power, P_{ran}, and the SEA matrix, C_{ran}, can be computed from the expressions

$$\text{Var}\left[P_{\text{ran},k}\right] = P_{\text{in},k}^2 r^2(\alpha_k, m_k') \quad \text{and} \tag{9}$$

$$\text{Var}\left[C_{\text{ran},ks}\right] = C_{ks}^2 r^2(\alpha_{ks}, m_k'), \tag{10}$$

where r^2 has the same form of equation (4) and m_k' is the effective modal overlap factor, which is equivalent to $1/C_{kk}^{-1}$, i.e. the inverse of the corresponding diagonal entry of the inverse SEA matrix **C**. The term α_k is related to the nature of the loading applied to the subsystem k, as previously defined, and α_{ks} is determined by the nature of the load exerted by the subsystem s to k. For line and area couplings $\alpha_{ks} = 2$. A detailed discussion about these parameters can be found in Refs. [11,12].

Variance of the energy density

It has been stated that the extended SEA approach can be used to estimate the variance of the total energy contained in a subsystem. However, it is not always possible to directly measure the total vibrating energy in the system, as a large number of sensors placed in several locations within the subsystem is required to average the response to calculate the total energy distributed in such subsystem. Therefore, it is of interest to estimate the variance of the energy density at a particular location. This issue has been addressed by Cotoni et. al. [12], and an expression to calculate the relative variance at a point, r_ϵ^2, has been derived based on conditional probability in the form of

$$r_\epsilon^2 = 1 + 2r_E^2, \tag{11}$$

where r_E^2 is the relative variance of the total energy. It is indicated that this result is an approximation only and the derivation is not rigorous, and more elaborated expressions can be found in the literature that consider the statistics of the mode shapes and the loading condition. However, the study carried out in Ref. [12] suggests that the use of equation (11) gives a good approximation between the experiments and the predictions.

Experimental setup

The prediction of structure-borne sound has several applications in the design of acoustic environments and noise control. For example, the sound pressure levels arising in a car cabin, due to structural vibrations, can be viewed as a random response in an ensemble of nominally identical vehicles from a production line. Such random behaviour, at high frequencies, might arise due to discontinuities in the material, changes on the shape of the structural components, variation in the manufacturing process, etc. As a case study, a built-up plate-cavity system has been designed to represent a scaled model of a flexible structural component of a vehicle and the acoustic cavity of the car cabin [16]. The criteria to scale the dimensions and the selection of the materials have been based on the number of the acoustic modes in a car cabin and the structural modes in a flexible panel, such as the roof panel, existing in a vehicle below 500 Hz. The scaled model is expected to match the number of modes, both acoustic and structural, at a higher frequency. The acoustic parameters such as speed of sound, air density and volume are presented in table 1, and the structural properties, such as Young's modulus, Poisson's ratio, density, area and thickness are shown in table 2.

Table 1. Acoustic properties.

Medium	c_0 [m/s]	ρ_0 [kg/m^3]	V [m^3]
Air	343	1.225	0.26

Table 2. Structural properties.

Component	E [GPa]	ν	ρ [kg/m^3]	A [m^2]	h [mm]
Brass plate	105	0.346	8470	0.49	0.5
MDF Walls	4	0.25	750	0.43 (larger) 0.31 (smaller)	54

The flexible brass plate has been randomised by placing ten masses of 22 g each on the top, corresponding to 10% of the total mass of the brass plate. In order to randomise the acoustic cavity, six rigid steel baffles have been randomly placed inside the box. Such baffles occupy less than 1% of the total interior volume, with a total surface of around 35% of the interior surface that encloses the acoustic cavity. The system is excited by a point-force exerted by a small hammer on a point of the brass plate. The out-of-plane response on the brass plate is measured by ten accelerometers placed at random locations on the plate, whereas the acoustic response is measured by a microphone placed inside the acoustic volume. The exterior view of the rig with the randomised plate is shown in figure 1. The interior of the cavity with the randomly distributed rigid baffles is schematically presented in figure 2.

SEA model of the structural-acoustic system

The SEA model here developed is intended to estimate the ensemble averaged response of the brass plate, and the arising sound pressure levels in the cavity due to the acoustic

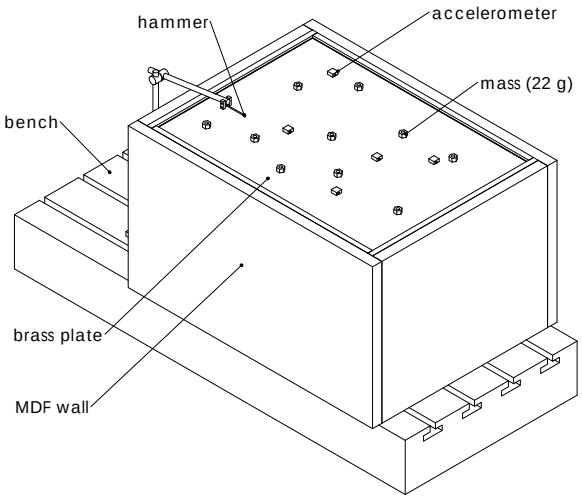

Figure 1. Exterior view of the test rig.

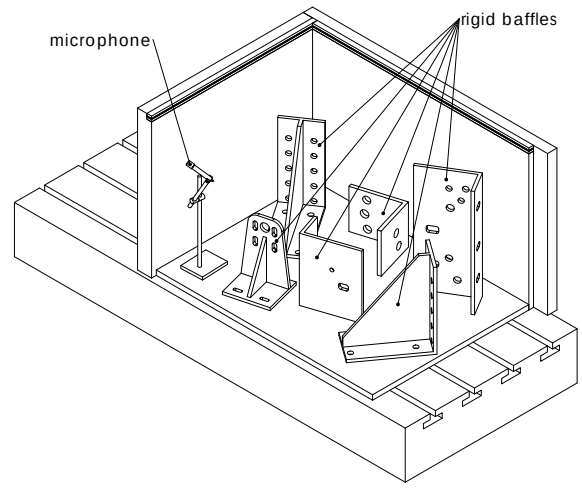

Figure 2. Interior of the acoustic cavity.

radiation of the coupled plate. It is assumed that most of the energy is contained in the flexible panel and the acoustic cavity, since the thick MDF walls are considerably more rigid. However, the walls of the box are also considered to be subsystems of the built-up system (the base is neglected, as it is fixed to a rigid bench). The parameters that appear on the equation (1) need to be determined prior the application of the SEA model.

Power input

The subsystem that receives the input power is the brass plate, since the force exerted on its surface generates bending waves that carry the energy to the coupled subsystems through the corresponding coupling interfaces. The input power can be expressed as

$$P_{\text{in}} = \frac{1}{2} |\text{F}|^2 \, \text{Re}\{\text{Y}_\text{m}\}, \tag{12}$$

where $|\text{F}|^2$ is the modulus squared of the complex force in the frequency domain and $\text{Re}\{\text{Y}_\text{m}\}$ is the real part of the mechanical mobility. As it is of interest to compute the response in the form of a transfer function, the modulus of the force is set to 1 N. The mechanical mobility of an infinite flat thin plate in out-of-plane motion (due to bending waves) has a real part only, and is equivalent to the inverse of the mechanical point impedance, i.e. $\text{Re}\{\text{Y}_\text{m}\} = 1/Z_p$, which depends on the geometry and the material properties of the plate [17].

Modal density

The modal density can be defined as the number of modes existing in a frequency band. Although this parameter can be computed analytically, for simple systems, or from numerical simulations; the SEA approach allows to describe the system in a much simpler form, and hence, asymptotic formulas are employed to calculate the modal densities of the subsystems comprising the SEA model.

The out-of-plane modal density of a flat thin plate is a constant that depends on the material properties and the geometry only, and is given by

$$n_{s_B} = \frac{\text{A}\sqrt{12}}{4\pi h c_L}, \quad \text{where } c_L = \left(\frac{\text{E}}{\rho(1-\nu^2)} \right)^{1/2}. \tag{13}$$

On the other hand, the asymptotic formulas for in-plane modal densities for longitudinal and shear waves are frequency dependent and given by

$$n_{s_L}(\omega) = \frac{\text{A}\omega}{2\pi c_L^2}, \quad \text{and} \tag{14}$$

$$n_{s_S}(\omega) = \frac{\text{A}\omega}{(1-\nu)\pi c_L^2}, \tag{15}$$

respectively. The strict definition of the modal density of a two-dimensional system includes an extra term to take into account the boundary conditions and the perimeter of the plate, however, for connected subsystems, the effective boundary conditions change with frequency and it is best to neglect this additional term [1].

For comparison, the out-of-plane mode count of both, the brass plate and the larger MDF wall of the box, have been computed by integrating equation 13, analytically from the natural frequencies of a simply supported rectangular thin plate with sinusoidal mode shapes, and numerically from an FE simulation performed in ABAQUS. Results are plotted in figure 3.

It can be seen in figure 3a that the asymptotic mode count of the brass plate is in good agreement with the analytical and numerical results. On the other hand, as shown in figure 3b, the asymptotic equation is not suitable for thick MDF walls, as these subsystems have a low mode count in the frequency band of interest, and are rather deterministic in the sense that the frequency spacings are much larger than the standard deviation of the natural frequencies, i.e. the statistic overlap is less than one. Hence, for the walls of the box, the results from an FE simulation where used instead.

Likewise, the acoustic modal density of a rectangular volume can be computed analytically from the natural frequencies [18], by an FE analysis or from the frequency dependent asymptotic formula given by

$$n_a(\omega) = \frac{V\omega^2}{2\pi^2 c_0^3} + \frac{S\omega}{8\pi c_0^2} + \frac{P}{16\pi c_0}, \tag{16}$$

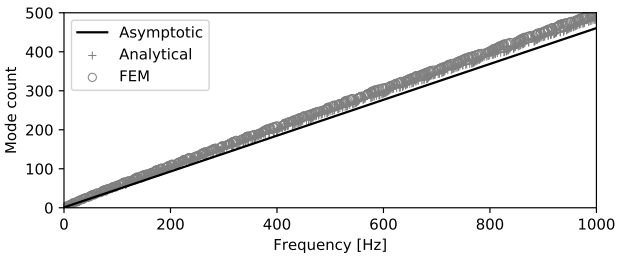

(a) Thin brass plate.

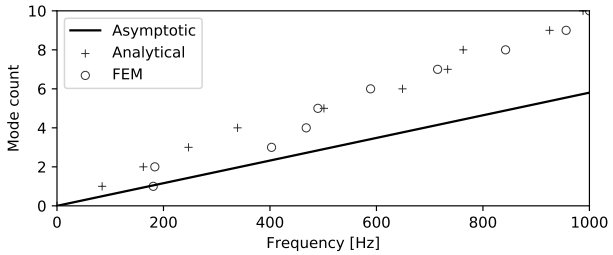

(b) Larger MDF wall.

Figure 3. Number of structural modes below 1 kHz. The modal density is the slope of the continuous line (equation 13).

where V is the volume, S is the area of the enclosing surface, P is the perimeter of the edges and c_0 is the speed of sound. There is also a good agreement between the acoustic mode count computed by integrating equation 16 and the acoustic mode count from analytical expressions or from an FE model, as it can be seen in figure 4.

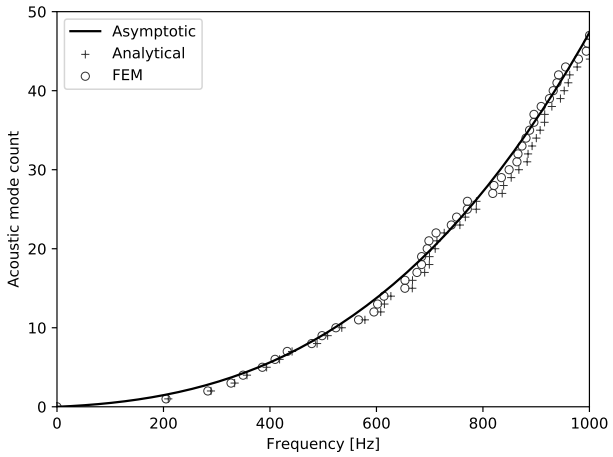

Figure 4. Number of acoustic modes below 1 kHz. The modal density is the slope of the continuous line (equation 16).

Line-type structural coupling

The coupling interface between two structural subsystems comprising the rig is line-type at a right angle, and the frequency dependent coupling loss factor can be expressed as a function of the diffuse wave transmission coefficients, $< \tau_{ij} >$ in the form

$$\eta_{ij} = \frac{2 c_B L < \tau_{ij} >}{\pi \omega A_i}, \quad \text{where } c_B = \left(\frac{h}{\sqrt{12}} c_L \omega \right)^{1/2}, \tag{17}$$

A_i is the area of the incident wave carrier plate, L is the length of the connection and c_L is the longitudinal wave speed, previously defined. The wave transmission coefficients can be calculated from the equations of motion on the coupling interface [19]. A plate carrying bending waves can also transmit longitudinal and shear waves to the coupled plate depending on the properties of the connection. Figure 5 shows the computed bending, longitudinal and shear wave transmission coefficients due to incident bending waves as function of frequency.

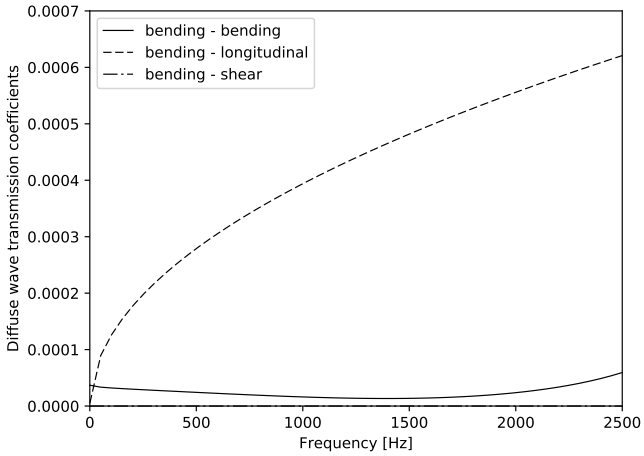

(a) Brass plate to MDF wall (bending-shear is close to zero)

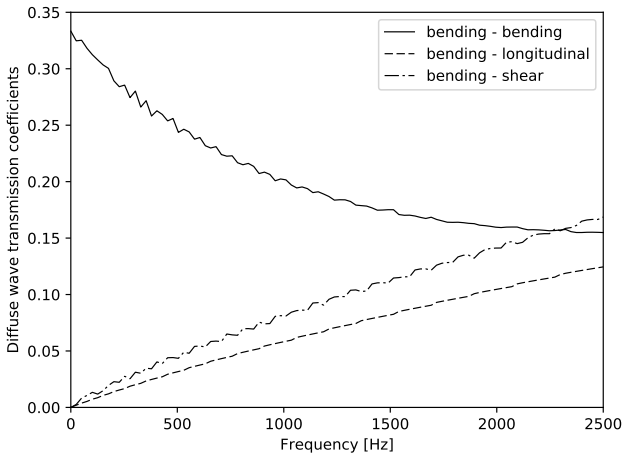

(b) MDF wall to MDF wall. The small oscillation are due to the numerical integration procedure over less data points to reduce the computing time, and will not affect the overall SEA results.

Figure 5. Diffuse wave transmission coefficients due to bending waves of the carrying subsystem.

The presence of bending, longitudinal and shear waves implies that each structural system contributes with three variables, i.e. modal energies, that must be computed simultaneously with the SEA equation, therefore the matrix $\mathbf{C}$ of this model has a dimension of 16×16, i.e. three variables of each of the five structural subsystems (one brass plate and four MDF walls) plus one variable of the acoustic cavity.

It is worth noting that the contribution of shear and longitudinal waves to the total vibrating energy of a structural system is smaller than the contribution of bending waves, since the in-plane modal densities are small compared to the

out-of-plane modal density, and therefore, neglecting the in-plane contribution, the number of variables can be reduced to six, i.e. a 6×6 $\mathbf{C}$ matrix. However, in this model the three types of waves were considered as the difference in computing time is not substantial.

Structural-acoustic coupling

The acoustic coupling can be expressed in terms of the radiation efficiency, σ, which is a dimensionless quantity that describes the rate of work done by the plate on the fluid of an acoustic medium. For a single-side radiation, the structural-acoustic coupling loss factor is given by

$$\eta_{ij} = \frac{\rho_0 c_0 \sigma}{\omega \rho h}, \tag{18}$$

where ρ_0 and c_0 are the air density and speed of sound, and ρ and h the density and thickness of the plate, respectively. The radiation efficiency can be computed from asymptotic formulas or by direct integration of the radiation equation presented by Leppington et al[20] for rectangular plates with freely hinged edges. It is known that this parameter at high frequencies asymptotically approaches to one, where the acoustic wave number is bigger than the wave number of the bending waves on the plate. In the opposite case, at lower frequencies, the radiation efficiency takes smaller values, and some discrepancies were found between the diffuse radiation efficiency computed from the integral form and from asymptotic formulas. Since the use of the integral equation is time consuming, an improved approach of integration was used to have a better estimation of the radiation efficiency of the structural subsystems in the model. Additionally, the authors in Ref.[21] have extended their work to include the effect of constrained edges in the computation of the radiation efficiency, and they have concluded that a correction factor of approximately 2 should be used below coincidence and 1 above, i.e. not altered. In this work, however, the initial formulation was used to estimate the radiation efficiency without any correction due to boundary conditions.

The range of frequencies of interest is in the region below the coincidence, i.e. the acoustic wave number is smaller than the corresponding bending wave number of the plate. The radiation efficiency of the structural components of the system is shown in figure 6, where it can be seen that the diffuse radiation efficiency takes its maximum value at the coincidence, which occur at high frequencies beyond the range of interest.

Loss factor

The structural loss factor can be better estimated from experimental data, since it was found that this parameter strongly depends on the frequency. Additionally, the random masses and accelerometers attached to the plate significantly increase the damping of the brass plate. The loss factor can be recovered from the logarithmic decrement of the amplitude of the bending waves at each frequency of interest. An impact test was performed on each isolated subsystem, i.e. brass plate and MDF walls, to record the response. A spectrogram of the time response was constructed to estimate the loss factor, due to internal damping and radiation losses, from the decaying spectrum in time.

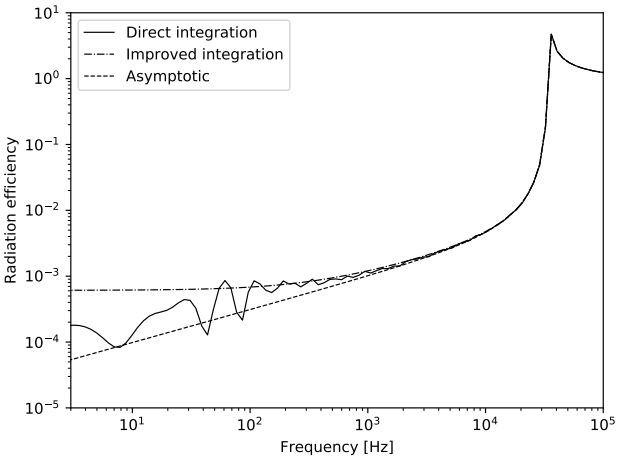

(a) Brass plate to acoustic volume.

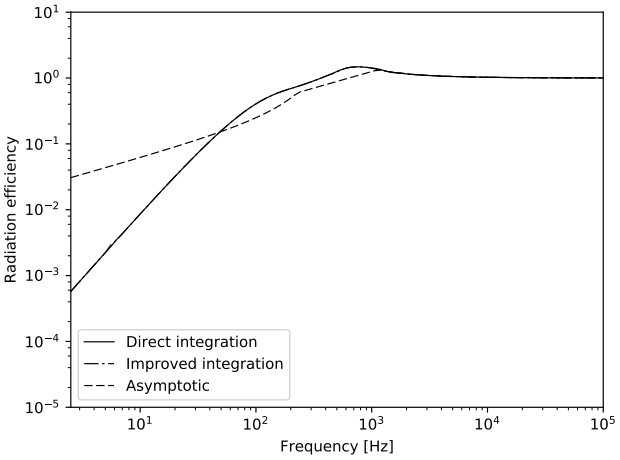

(b) MDF wall to acoustic volume ('Improved integration' line is overlapped to the 'Direct integration' line)

Figure 6. Acoustic radiation efficiency.

As it is difficult to obtain reliable data of the decays of the acoustic waves at several frequencies after a single test, the acoustic volume, enclosed with rigid walls to avoid any coupling losses, was excited with a pure tone coincident with a particular resonance frequency, and the acoustic loss factor was extracted from the time decay of the wave. The frequency dependent loss factors of each of the subsystems are presented in figure 7.

It can be observed that the structural loss factor can be approximately fitted to an exponential function of the frequency. The coefficient of determination R^2 calculated for the brass plate is 0.88 without randomisation, and 0.75 when randomised. For the MDF wall, R^2 is 0.79. On the other hand, the magnitude of the acoustic loss factor seems to be more frequency-dependent at lower frequencies than at higher, since over around 1 kHz its magnitude approaches to a constant value. An exponential fitting gives a R^2 of 0.64, whereas for a polynomial fitting R^2 is 0.92.

Dynamic quantities from energy estimation

In order to compare the predicted energy levels with experimental data, it is useful to express the energy of the structural subsystems in terms of averaged displacement or velocity. In the frequency domain, the ensemble averaged

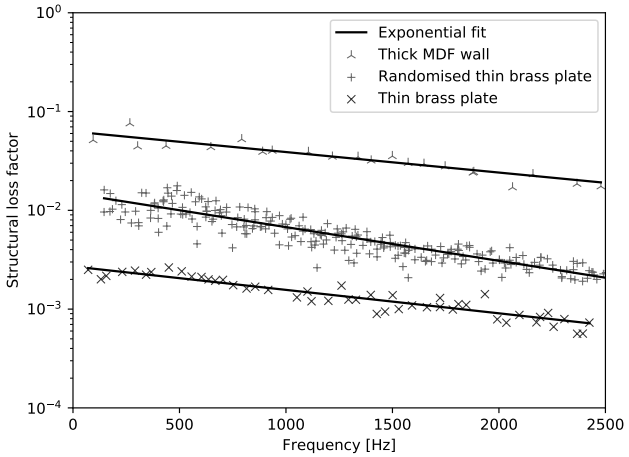

(a) Structural loss factor.

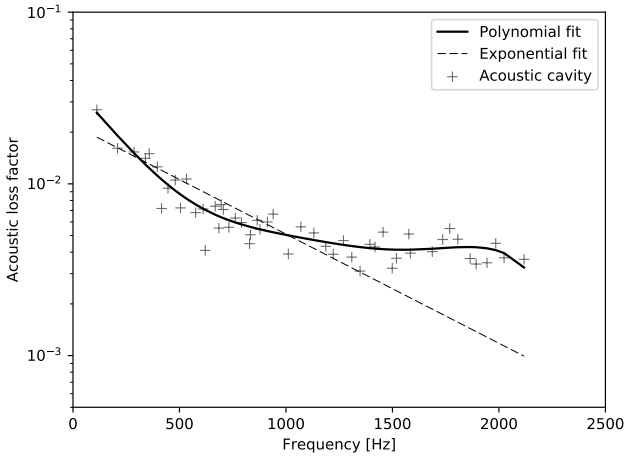

(b) Acoustic loss factor.

Figure 7. Experimental loss factors and data fitting lines.

squared velocity is proportional to the mean energy and expressed as

$$\mathrm{E}\left[|v_{\mathrm{SEA}}|^2\right] = \frac{2\mathrm{E}[E]}{M}, \tag{19}$$

where $\mathrm{E}[E]$ and M are the predicted ensemble averaged energy and the mass of the brass plate, respectively. The factor of 2 is omitted if the velocity v_{SEA} is expressed as RMS. Since the energy was estimated for a unitary input force, the modulus squared of the velocity in equation (19) represents the force-velocity transfer function.

The predicted averaged acoustic pressure levels is also proportional to the mean energy of the cavity and can be computed from

$$\mathrm{E}\left[|p_{\mathrm{SEA}}|^2\right] = \mathrm{E}[E]\rho_0 c_0^2/V, \tag{20}$$

where ρ_0, c_0 and V are the air density, speed of sound and volume, respectively, and $\mathrm{E}[E]$ is the predicted ensemble averaged energy of the acoustic cavity. Likewise to equation (19), the modulus squared pressure in equation (20) is the force-pressure transfer function.

Comparison with experimental results

An individual test performed on the rig consist of exciting the brass plate with an instantaneous point force exerted by a hammer equipped with a force transducer. The out-of-plane response on the brass plate measured by the accelerometers was recorded in 0.4 s. Since the system is linear, the Fourier transform of the time data of the excitation and the response, as well as the transfer function, are independent on the length of the recording. Additionally, the recording time is enough for the signal to fully decay. Therefore, the steady-state, rather than transient, formulation of the SEA presented in this paper is used to estimate the averaged response of the system.

The experimental data has been expressed in terms of velocity rather than acceleration. The complex force-velocity transfer functions can be computed from the acceleration-force cross-spectrum, S_{af}, and force auto-spectrum, S_{ff}. It was found that the mass of the accelerometer affects the measurements of the response of the flexible system due to its impedance. Therefore a correction factor C_Z that accounts for the effect of the local impedance in the response is applied. The squared modulus of the force-velocity transfer function of the brass plate is evaluated as

$$\left|v_{\mathrm{exp}}\right|^2 = C_Z \left|\frac{S_{af}}{S_{ff}}\right|^2 \frac{1}{\omega^2}, \quad \text{where} \quad C_Z = \left|\frac{Z_p + Z_a}{Z_p}\right|^2, \tag{21}$$

Z_p is the point impedance of the plate and Z_a is the impedance of the accelerometer. Neglecting any effect of the attachment of the accelerometer to the plate, the impedance of the accelerometer is $Z_a = \mathrm{j}\omega M_a$, where M_a is the mass of the accelerometer, i.e. 22 g.

The time series data recorded by the microphone inside the acoustic volume is processed to express the sound pressure levels in the frequency domain. The force-pressure transfer functions were computed from the pressure-force cross-spectra, and force auto-spectrum, therefore, the modulus squared of the pressure levels to a unit force is

$$\left|p_{\mathrm{exp}}\right|^2 = \left|\frac{S_{pf}}{S_{ff}}\right|^2. \tag{22}$$

A data set has been collected after multiple realisations, each consisting of an individual test performed for a particular distribution of the masses on the plate and position of the baffles in the acoustic cavity.

Randomised plate coupled to a deterministic acoustic cavity

Modelling a system with an SEA approach requires that all of the components have a statistical behaviour rather than deterministic. However, it is noted from equation (8) that the estimation of the variance of energy depends on the statistics of the power input and the random SEA matrix. In order to verify the effect of the power transmitted from a random structural subsystem to a coupled deterministic cavity in the computation of the variance of energy, a set of multiple realisations has been collected for twenty different mass distributions on the plate for a unique configuration of the acoustic volume*. The comparison between the experimental

*Five nominally identical tests were performed for each random distribution of the masses on the brass plate.

mean response and the SEA predictions are plotted in figure 8. The experimental and predicted relative variance of energies are shown in figure 9.

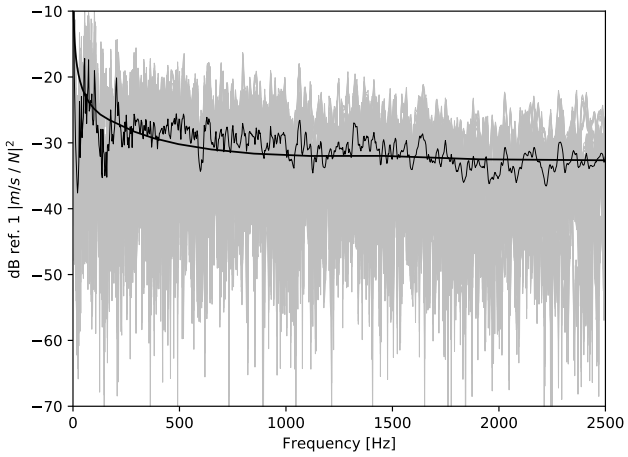

(a) Modulus squared velocity of the randomised brass plate.

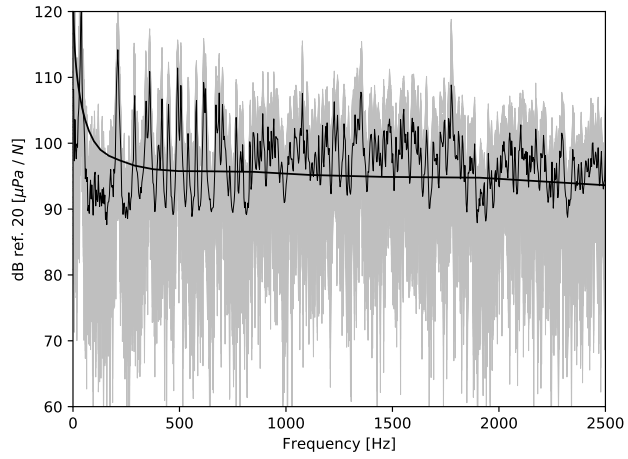

(b) Sound pressure levels in the deterministic acoustic cavity.

Figure 8. Dynamic response of the randomised brass plate and the coupled deterministic acoustic cavity due to a point-force excitation on the plate. Gray: response of each individual realisation; fluctuating black: experimental average; continuous black: SEA estimation.

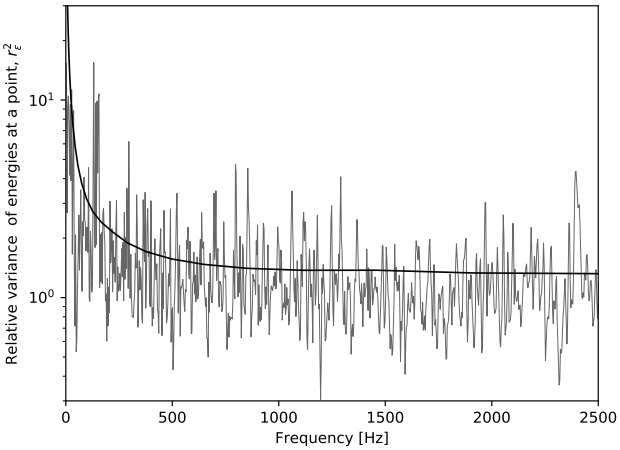

(a) Randomised brass plate.

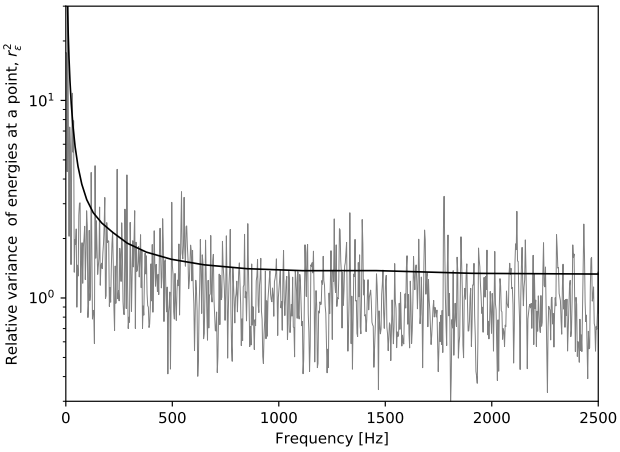

(b) Deterministic acoustic cavity.

Figure 9. Relative variance of energies at a point. Fluctuating: experimental data; continuous black: SEA prediction.

As it was expected, in figure 8a, the experimental mean response of the random subsystem, i.e. the randomised brass plate, agrees fairly well with the SEA estimation. On the other hand, as shown in figure 8b, the SEA estimation of the acoustic response seems to be under-predicted in the order of 5 to 10 dB, and the fluctuations around the mean are significantly large, compared to the 'smoother' experimental mean response of the randomised brass plate. This apparent under-prediction of the acoustic response, is found to be due to two issues. First, there is a lack of individual samples to average, as it will be further demonstrated when more individual samples were collected for the randomised acoustic cavity. Second, it is assumed that the acoustic field inside the cavity is diffuse, however, acoustic measurements for this set of experiments were taken from a particular location and therefore diffusivity is not ensured. Since the microphone was placed close to the lateral wall and near to one of the edges, it is expected and under-prediction between 3 to 6 dB, as explained in Ref.[22] This issue is addressed in the next subsection where acoustic measurements were taken at several locations within the acoustic volume.

Since the variance of the acoustic energy was computed considering that the term r^2 of the variance of the random matrix is zero, due to the deterministic nature of the cavity, the relative variance of the acoustic energy is expected to be close to the corresponding relative variance of energy of the brass plate. It can be seen that the experimental variance of the randomised brass plate, plotted in Fig 9a, is in the same order of magnitude of the variance of the deterministic acoustic cavity, shown in figure 9b; however, although the SEA estimation has the same tendency as the experimental variance, it is over-predicted. Additionally, at several frequencies within the range, the experimental relative variance at a point is lower than the one, which is in contradiction with the theory, as described by equation (11). It is demonstrated further in this section, that the reason for the discrepancy is that the number of samples here considered do not form a sufficiently large ensemble, and the agreement is improved when a larger number of realisations have been performed for different random configurations.

Randomised plate coupled to a randomised cavity

The acoustic cavity was further randomised by placing the rigid baffles at arbitrary positions within the volume. Ten different configurations of the mass distribution on the brass plate were tested for each of the ten random positions of the baffles inside the cavity, making an ensemble of one hundred different random structural-acoustic configurations.[†] The mean response of the randomised brass plate and acoustic cavity are plotted in figure 10.

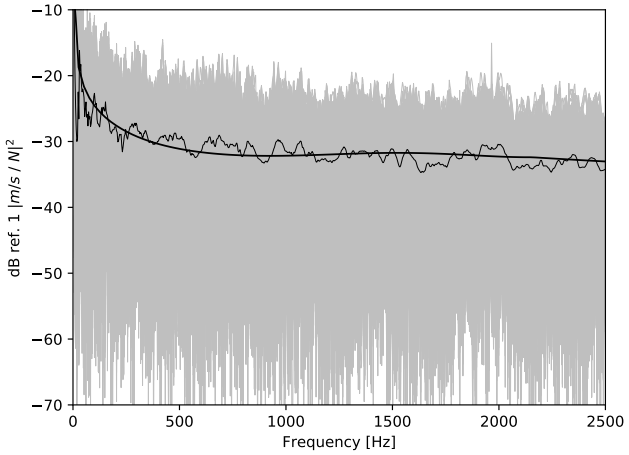

(a) Modulus squared velocity of the randomised brass plate.

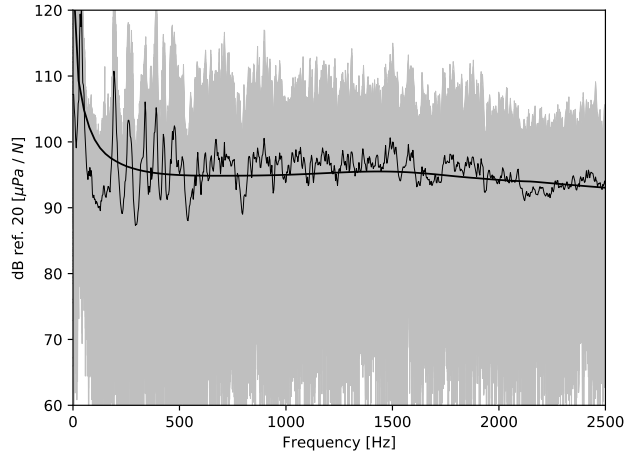

(b) Sound pressure levels in the randomised acoustic cavity.

Figure 10. Dynamic response of the random structural-acoustic system due to a point-force excitation on the plate. Gray: response of each individual realisation; fluctuating black: experimental average; continuous black: SEA estimation.

It can be seen in figure 10a that the mean response of the brass plate is well estimated by the SEA model, as the fluctuations of the experimental mean around the predicted are less than 2 dB. The good agreement between the experimental and predicted mean structural response was expected as the brass plate was randomised a total of one hundred times. Regarding the mean acoustic energy, it can be seen on figure 10b that the response is rather deterministic at frequencies below 600 Hz since few acoustic modes are found below that frequency, however, the fluctuation of the experimental mean is significantly lower at higher frequencies and the agreement with the SEA estimation is better with a fluctuation less than 4 dB. Since ten random acoustic configurations were tested, it can be expected that the mean acoustic response of a larger ensemble, i.e. more realisations with further randomisation of the acoustic cavity, will be in better agreement as the tendency of the prediction match well with the observed experimental data.

The experimental variance of energy at a point of the random brass plate, was calculated from the data collected from one of the accelerometers placed on the top of the plate, whereas the variance of the total energy was computed from the data collected from ten accelerometers placed on different positions on the plate. The experimental and SEA variance for the brass plate are shown on figure 11.

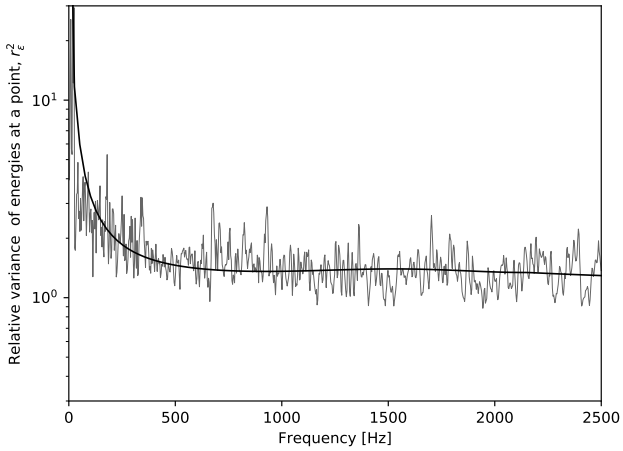

(a) Relative variance of the energy density at a point. Data from one accelerometer on the plate. SEA estimation with equation 11.

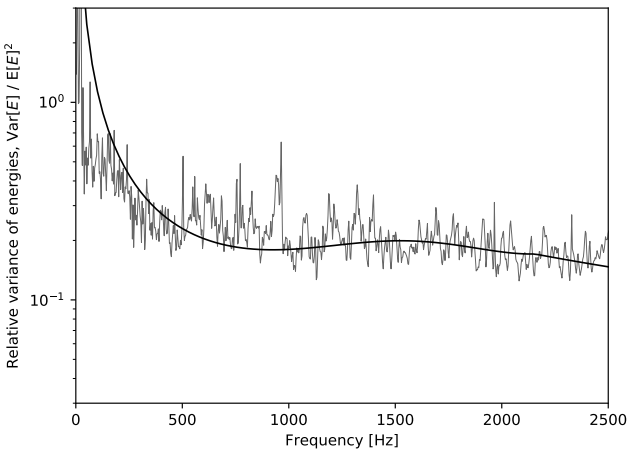

(b) Relative variance of the total energy. Data from ten accelerometers distributed on the plate.

Figure 11. Relative variance of energy of the brass plate. Fluctuating: experimental data; continuous black: SEA prediction.

It is observed that the estimated SEA variance of energies at a point, figure 11a, agrees remarkably well with the experimental variance of the response of the brass plate. It is noted that the experimental variance is greater than one at

[†]Five nominally identical tests were performed for each random structural-acoustic configuration.

every frequency within the range of interest, which confirms that the discrepancy observed in figure 9a was due to an insufficient number of realisations. As shown in figure 11b, the agreement is also good between the predicted variance of total energy and the experimental variance computed from the data gathered from the ten accelerometers placed on the plate. This result suggests that the number of measuring points was enough to have a reliable estimation of the experimental variance of the total energy of the brass plate. With a lower number of accelerometers, the experimental variance was observed to be above the SEA prediction.

The data to compute the relative variance of the acoustic response at a point were collected from a microphone placed in a particular location within the cavity. To calculate the experimental variance of the total acoustic energy of the cavity, further realisations where performed to collect data with the microphone placed at several arbitrary locations within the randomised volume. Two further experimental data sets were collected. The first data set consists of the acoustic response measured in three different locations after fifty realisations, when the acoustic cavity was randomised ten times. The second data set consists of the acoustic response data of twenty-five realisations, and measurements were taken at six different locations in the cavity that was randomised five times[‡]. The comparison between the experimental variance and the SEA prediction can be seen on figure 12.

Due to the deterministic nature of the cavity at lower frequencies, the SEA results are only expected to be reliable at frequencies above 600 Hz. It can be seen on figure 12a that the SEA estimation approximates fairly well the experimental relative variance at a point. Additionally, the ten random acoustic configurations, with the corresponding number of randomisations of the brass plate, were sufficient to demonstrate that the experimental relative variance of acoustic energy at a point is above one, as it would have been expected from the Schroeder statistics at higher frequencies[5]. The experimental variance of the total energy, calculated with data gathered from fifteen different acoustic random configurations and nine measuring points, is found to have the a good agreement with the SEA prediction plotted in figure 12b.

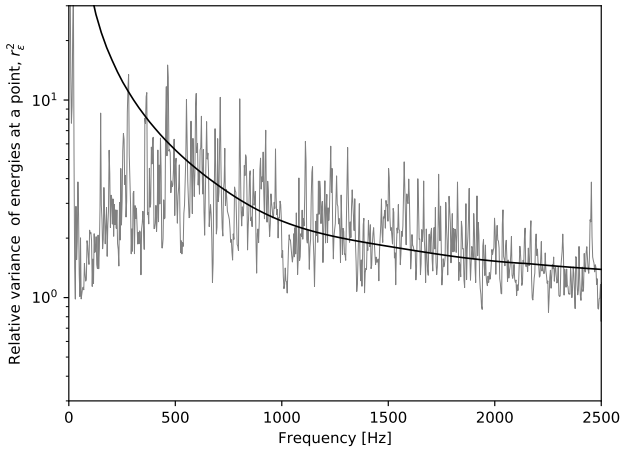

(a) Relative variance of the energy density at a point. Data from the microphone placed at a particular location within the volume. SEA estimation with equation 11.

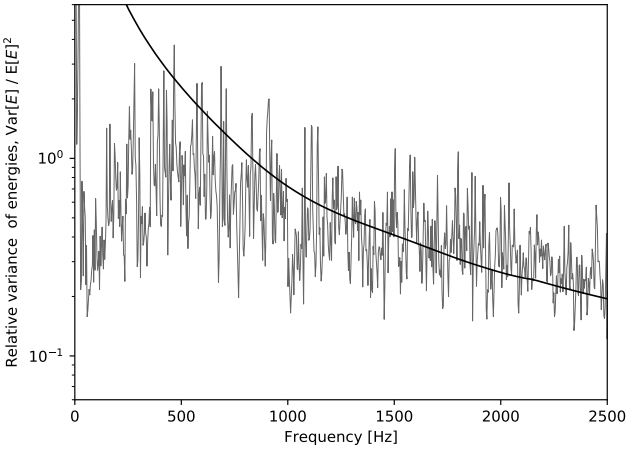

(b) Relative variance of the total energy. Data from the microphone placed in a total of nine arbitrary locations within the volume.

Figure 12. Relative variance of energy of the acoustic cavity . Fluctuating: experimental data; continuous black: SEA prediction.

Conclusions

In the present work, the extended SEA analysis based on the GOE statistics has been applied to estimate the statistical response of a structural-acoustic system. As no previous works have been made regarding to the experimental validation of the higher statistics of coupled structural-acoustic systems, a novel feature in this work is that this case study constitute a supporting evidence that the variance of the acoustic energy arising from the vibrations of a coupled structural subsystem can be reliably estimated using a GOE based model.

The advantage of an SEA approach to analyse complex systems is that the averaged response and variance can be rapidly estimated form relatively simple expressions, whereas the computation of the averaged structural and acoustic response of physical systems requires a large ensemble of random nominally identical systems, as well as measurements in several locations within the system. A good agreement is found between SEA estimations and experimental mean and variance in the frequency range where there is a high degree of statistical overlap, and therefore poor agreement is found at lower frequencies, when the system is rather deterministic with a statistical overlap less than one.

Acknowledgements

This work has been sponsored by Bose Corporation. Luis Andrade A. would like to gratefully acknowledge the financial support from SENESCYT-Ecuador to fund his doctoral studies.

[‡]For both data sets, each acoustic random configuration was tested with five different mass distribution on the brass plate. Three nominally identical test were performed.

References

1. Lyon RH and DeJong RG. *Theory and application of statistical energy analysis*. Newton MA: Butterworth - Heinemann, 1995.
2. Langley RS. A general derivation of the statistical energy analysis equations for coupled dynamic systems. *Journal of Sound and Vibration*. 1989 Dec 22;135(3):499-508.
3. Bernhard RJ. The Limits of Predictability due to Manufacturing and Environmentally Induced Uncertainty. In: *International Congress on Noise Control Engineering INTER-NOISE 96*, Liverpool, UK, 30 July - 2 August 1996, pp. 2867-72. St Albans: Institute of Acoustics.
4. Norton MP and Karczub DG. *Fundamentals of noise and vibration analysis for engineers*. Cambridge university press; 2003 Oct 16.
5. Schroeder MR. Frequency-correlation functions of frequency responses in rooms. *The Journal of the Acoustical Society of America*. 1962 Dec;34(12):1819-23.
6. Lyon RH. Statistical analysis of power injection and response in structures and rooms. *The Journal of the Acoustical Society of America*. 1969 Mar;45(3):545-65.
7. Davy JL. The ensemble variance of random noise in a reverberation room. *Journal of Sound and Vibration*. 1986 Jun 22;107(3):361-73.
8. Langley RS and Brown AW. The ensemble statistics of the energy of a random system subjected to harmonic excitation. *Journal of Sound and Vibration*. 2004 Aug 23;275(3-5):823-46.
9. Langley RS and Brown AW. The ensemble statistics of the band-averaged energy of a random system. *Journal of Sound and Vibration*. 2004 Aug 23;275(3-5):847-57.
10. Manohar CS and Keane AJ. Statistics of energy flows in spring-coupled one-dimensional subsystems. *Phil. Trans. R. Soc. Lond.* 1994 Mar 15;346(1681):525-42.
11. Langley, RS and Cotoni V. Response variance prediction in the statistical energy analysis of built-up systems. *The Journal of the Acoustical Society of America*. 115.2 (2004): 706-718.
12. Cotoni V, Langley RS and Kidner MR. Numerical and experimental validation of variance prediction in the statistical energy analysis of built-up systems. *Journal of Sound and Vibration*. 2005 Dec 6;288(3):701-28.
13. Jacobsen F and Rodriguez Molares A. The ensemble variance of pure-tone measurements in reverberation rooms. *The Journal of the Acoustical Society of America*. 2010 Jan;127(1):233-7.
14. Fahy FJ and Gardonio P. *Sound and structural vibration: radiation, transmission and response*. Elsevier; 2007 Jan 12.
15. Abramowitz M and Stegun IA. *Handbook of mathematical functions: with formulas, graphs, and mathematical tables*. Dover Publications, 1964.
16. Andrade L, et al. Experimental validation of the statistics of a structural-acoustic system for active noise control applications in vehicles. In: *The* 6^{th} *conference of Noise and Vibration Emerging Methods NOVEM*, Ibiza, Spain, 7-9 May 2018, paper no. NVC1 171812, pp. 1-12, Barcelona: Universitat Ramon Llull La Salle.
17. Cremer L, Heckel M and Petersson, BAT. *Structure-borne sound*. 3rd ed. Berlin: Springer; 2005.
18. Blevins RD. Modal density of rectangular volumes, areas, and lines. *The Journal of the Acoustical Society of America*. 2006 Feb;119(2):788-91.
19. Langley RS and Heron KH. Elastic wave transmission through plate/beam junctions. *Journal of Sound and Vibration*. 1990 Dec 8;143(2):241-53.
20. Leppington FG, Broadbent EG and Heron KH. The acoustic radiation efficiency of rectangular panels. *Proc. R. Soc. Lond. A 382*. 1982 Aug 9;382(1783):245-71.
21. Leppington FG, Broadbent EG and Heron KH. Acoustic radiation from rectangular panels with constrained edges. *Proc. R. Soc. Lond. A 393*.1984 May 8;393(1804):67-84.
22. Jacobsen F. The sound field in a reverberation room. Report, Technical University of Denmark, Lyngby, Denmark. 2011.